GGA + U study of the electronic energy bands and state density of the wurtzite $In_{1-x}Ga_xN$*

Wang Wei-Hua(王伟华)[a], Zhao Guo-Zhong(赵国忠)[a)b)†], and Liang Xi-Xia(梁希侠)[a]

[a] *Department of Physics, Inner Mongolia University, Hohhot* 010021, *China*
[b] *Department of Physics, Capital Normal University, Beijing* 100048, *China*

(Received 8 March 2013; revised manuscript received 8 May 2013)

The electronic band structures, densities of states (DOSs), and projected densities of states (PDOSs) of the wurtzite $In_{1-x}Ga_xN$ with $x = 0$, 0.0625, 0.125 are studied using the generalized-gradient approximation (GGA) and GGA + U in density functional theory. Our calculations suggest that in the case of wurtzite InN it is important to apply an on-site Hubbard correction to both the d states of indium and the p states of nitrogen in order to recover the correct energy level symmetry and obtain a reliable description of the InN band structure. The method is used to study the electronic properties of the wurtzite $In_{1-x}Ga_xN$. The conduction band minimum (CBM) energy increases, while the valence band maximum (VBM) energy decreases with the increase of the gallium concentration. The effect leads to broadening the band gap (BG) and the valence band width (VBW). Furthermore, the compressive strain in the crystal can cause the BG and the VBW to increase with the increase of gallium concentrations.

Keywords: GGA + U, electronic structures, projected density of states, $In_{1-x}Ga_xN$

PACS: 02.60.Cb, 03.75.Hh **DOI:** 10.1088/1674-1056/22/12/120205

1. Introduction

III-nitride wurtzite ternary alloys have attracted more attention because of their potential applications in optical devices.[1,2] The ternary compound $In_{1-x}Ga_xN$ has the great potential for numerous applications such as light emitting diodes (LEDs), laser diodes (LDs), and transistors.[3] Shan *et al.*[4] have studied the optical properties of $In_xGa_{1-x}N$ alloys grown by metallo-organic chemical vapor deposition. Aschenbrenner *et al.*[2] studied optical and structural characteristics of AlInN layers by ellipsometric measurements and high resolution x-ray diffraction. Sanford *et al.*[5] studied the refractive indices and birefringences of $In_xGa_{1-x}N$ films by prism coupling used in conjunction with multilayer optical waveguide analysis. $In_{1-x}Ga_xN$ has aroused substantial interest as a photoelectrode material for several reasons, the most important being that the band gap can be tuned over a wide spectral range from the visible to the ultraviolet regime of the electromagnetic spectrum and $In_{1-x}Ga_xN$ alloys are corrosion resistant.[6]

From a theoretical point of view, the density functional theory (DFT), including the local density approximation (LDA) and the generalized gradient approximation (GGA) can be used to study the structural, electronic, and optical properties of the wurtzite $In_{1-x}Ga_xN$. However, these methods underestimate the $In_{1-x}Ga_xN$ band gap, giving rise to zero or negative values. The hybridization between the cation semicore d states and the anion p valence states is overestimated.[7] As a result, the valence band maximum (VBM) is pushed toward higher energies, reducing the $In_{1-x}Ga_xN$ energy gap. Furthmüller *et al.*[8] studied the electronic structure of the wurtzite InN in the quasiparticle aspect with the GW approximation.[8] However, this procedure is computationally demanding so that it is difficult to apply the procedure to complex systems such as the alloys studied here. Maurya *et al.*[9] studied the electronic and optical properties of InN by DFT within Engel–Vosko's corrected GGA method. As far as we know, the details of the electronic structural properties of $In_{1-x}Ga_xN$ have not been studied.

In this work, to recover the main InN band features and to correct the deficiency of GGA in describing the Coulomb interaction between localized states, we use the GGA + U[10] method and apply a Hubbard U[11] correction to both the d electrons of the cation (indium) and the p electrons of the anion (nitrogen).[12] In the following, we will denote this computational scheme as GGA + U. Moreover, the electronic structural properties of the wurtzite $In_{1-x}Ga_xN$ as found using the GGA + U method, are discussed in detail.

2. Theoretical methods

The electronic band structures, the density of states (DOS), and the projected density of states (PDOS) of the wurtzite $In_{1-x}Ga_xN$ were studied using the generalized-gradient approximation (GGA) and GGA + U in density func-

*Project supported by the National Natural Science Foundation of China (Grant No. 50971094), the Natural Science Foundation of Beijing, China (Grant Nos. KZ201310028032 and 1092007), and the Domestic Visiting Program for the Graduate Students of Inner Mongolia University, China.

†Corresponding author. E-mail: guozhong-zhao@126.com

© 2013 Chinese Physical Society and IOP Publishing Ltd

tion theory (DFT). The GGA with exchange–correlation function and ultrasoft pseudopotential terms were used with taking into account the In–4d and Ga–3d electronic states.[13] The DFT calculations were performed using the PWSCF program.[14] In order to keep the calculation precision, the plane-wave cutoff energy was set to be 45 Ry (1 Ry = 13.605 eV). The numerical integration of the Brillouin zone (BZ) was performed using a k-mesh of dimensions 4×4×4. Convergence with respect to the plane-wave cutoff energy and k-point sampling was carefully checked. For the lattice constant of bulk InN, a and c were set respectively to be 3.538 Å and 5.703 Å, as obtained from the experiment.[15] All of the internal structural parameters of the wurtzite InN were optimized by minimizing the total energy using the quasi-Newton algorithm. The electron occupation number was determined by the Methfessel–Paxton (MP) method.[16] Moreover, the electronic configurations In–4d 5s, 5p, Ga–3d, 4s, 4p, and N–2s, 2p in the cell are considered in our calculations.

To model the wurtzite $In_{1-x}Ga_xN$ ternary alloys, we used a 32-atom supercell with periodic boundary conditions in Material Studio (MS)[17] as shown in Fig. 1. This corresponds to a 2×2×2 supercell which is twice the size of the primitive wurtzite unit cell in both directions, along the basal plane and along the c axis. The gallium concentrations $x = 0$, 0.0625, 0.125 were realized by substituting 0, 1, and 2 indium atoms by gallium atom in a 32-atoms supercell. For each value of x, the $In_{1-x}Ga_xN$ structure can be optimized as different supercells to find the equilibrium volume to satisfy the principle of minimizing the total energy.

The GGA + U[10] method differs from the GGA method by an extra term (E_U) that is added. E_U corresponds to the mean-field approximation of the Coulomb interaction in the multiband Hubbard model where U[11] represents the screened Coulomb parameter. It is defined as the local potential to be applied to the selected atomic species. The GGA + U method aims to correct the description of the Coulomb interaction only among highly correlated states, such as d or f.[18] Since the interaction between N–2p and In–4d electrons results in the narrowing of the band-gap, the addition of a Hubbard term to d electrons is expected to lower their energy, resulting in an increase in band-gap. Here we denote a Hubbard term for d electrons as U_d and for p electrons as U_p.[12] Including the U correction on the anion seems to be fundamental to a better description of p–d interaction in InN, similar to previous observations for certain oxide compounds.[19] Besides inducing the increase of band-gap, it corrects the symmetry of states near the top of the valence band.

A major issue when performing GGA + U calculations is the choice of the U parameter, which is often evaluated by trying to reproduce experimental photoemission data. In this work, the U_d and U_p are systematically changed to examine their effects on the position of the 4d band of indium, on the position of the 2s states of nitrogen, on the VBW and the electronic band gap at Γ point. In Ref. [20], the following experimental values were presented: the 4d states of indium were found to be at about 16 eV below the VBM, the nitrogen 2s band 12 eV below the VBM, VBW about 6.4 eV, and energy gap about 0.7 eV. Our examining values of U_d and U_p were varied to give the results close to these experimental values, thereby obtaining the optimized values of $U_d = 6.0$ eV and $U_p = 3.5$ eV.

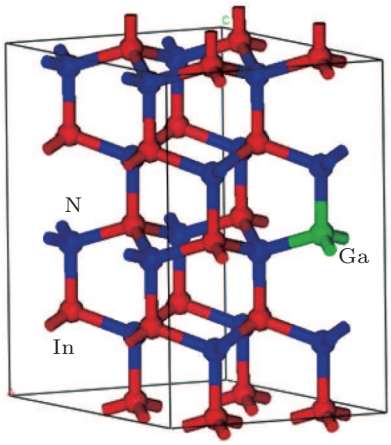


Fig. 1. (color online) Schematic of the supercell (2×2×2) of wurtzite $In_{0.9375}Ga_{0.0625}N$.

3. Results and discussion

3.1. Electronic band structure of InN

In Fig. 2, the electronic band structures of the wurtzite InN obtained with GGA (a) and GGA + $U^{(d+p)}$ (b) are compared. It can be seen that GGA + $U^{(d+p)}$ induces a gap opening at Γ as 0.78 eV. The In–4d band is centered at about 16 eV below the VBM, while the N-2s band energy is shifted down by about 0.5 eV with respect to GGA. Correspondingly, the VBW is increased to about 6.24 eV, which is very close to the values obtained by the experiment and by the many-body corrections (G_0W_0).[21] The energy of CBM increases with Ga concentration increasing, while the energy of VBM decreases. The effect leads to broadening the band gap and the valence band. The values of the band gap, valence band width and lattice constants for the wurtzite InN with GGA and GGA + $U^{(d+p)}$ are given and are compared with previous calculations and the experimental data in Table 1.

In previous calculations, the LDA predicts a negative sp band gap.[22] Regardless of the chosen U_d value,[18] this deficiency is not corrected by applying a U correction to the d states of indium. Including the U term on both the d electron of indium and p electron of nitrogen, however, this problem

is resolved and so the correct energy gap at the Γ point can be predicted. The GGA + $U^{(d+p)}$ in Fig. 2(b) not only induces a gap opening about 0.78 eV at Γ point, but also predicts the correct energy ordering near the VBM, giving rise to two degenerate p states at the top of the valence band and one *s* state at the bottom of the conduction band. InN is then confirmed as the semiconductor (GGA + $U^{(d+p)}$) rather than the conductor (GGA).

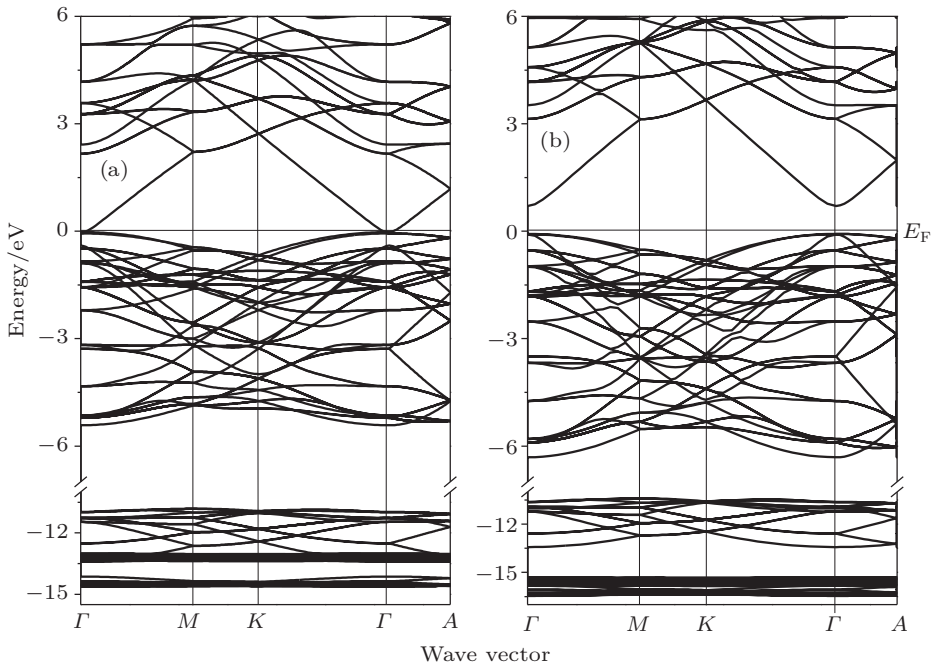


Fig. 2. Band structures of the wurtzite InN obtained with GGA (a) and GGA + $U^{(d+p)}$ (b).

Table 1. Values of band gap, up-valence band, low-valence band, and the lattice parameters *a*, *c* for the wurtzite InN ($x = 0$).

x	Band gap/eV	Up-valence band/eV	Low-valence band/eV	a/Å	c/Å
GGA	0.0125	5.42	3.594	3.64	5.85
GGA + $U^{(d+p)}$	0.78	6.24	5.83	3.56	5.73
Other Calc.	–0.36[a] –0.27[b]	5.77[c] 5.993[d]		3.59[e] 3.541[d]	5.81[e] 5.683[d]
Exp.	0.69[f] 0.7	6.0[g] 6.4		3.538	5.703

[a]Ref. [23], [b]Ref. [24], [c]Ref. [25], [d]Ref. [26], [e]Ref. [27], [f]Ref. [28], [g]Ref. [29].

3.2. Electronic band structure of $In_xGa_{1-x}N$

Figure 3 shows the variations of calculated lattice parameters of $In_{1-x}Ga_xN$ with gallium content x. For the $In_{1-x}Ga_xN$ alloys, the lattice constant c shows a linear variation with Ga concentration, but a small deviation from Vegard's law is clearly visible for the lattice constant a, where there is an downward bowing. This deviation is due to the relaxations of the In–N and Ga–N bond lengths in $In_{1-x}Ga_xN$.

The electronic band structures with different values of concentration x of Ga in the wurtzite $In_{1-x}Ga_xN$ with GGA and GGA + $U^{(d+p)}$ are shown in Fig. 4. It shows the direct band-gap nature at the Γ point, with a new energy state appearing in the 3.15 eV–4.29 eV which is the degeneracy of the states in pure InN and lifted due to the introduction of Ga. As is well known, the density-functional theory underestimates the band gap, thus leading to the band gap values of In–4d and Ga–3d electronic state for $In_{1-x}Ga_xN$ in our calculation being smaller than the experimental results and close to zero, which also accords with previously theoretical calculations.[26] However, the results of GGA + $U^{(d+p)}$ show remarkable agreement with experimental data. The values of the band-gap, valence band width and lattice constants for $In_{1-x}Ga_xN$ are given in Table 2.

Additionally, with increasing Ga concentration in $In_{1-x}Ga_xN$, the band-gap and valence-band width are increased as shown in Fig. 3. The variation tendency is consistent well with the experimental result.[30] Especially, the lattice constants decrease with increasing Ga content x due to the gallium radius being smaller than the indium radius. Thus, the higher compressive strain in the crystal structure gives rise to

the band gap and the valence band width increases with gallium content increasing. We have fitted these data by the polynomial fitting for the lattice parameter, a and the linear fitting for the lattice parameter c, each as a function of gallium content x. The fitting formulae of the lattice parameter a and c are as follows:

$$a = 0.64x^2 - 0.488x + 3.56, \quad (1)$$

$$c = -0.584x + 5.735, \quad (2)$$

which can be used to obtain the lattice parameters for the different values of x.

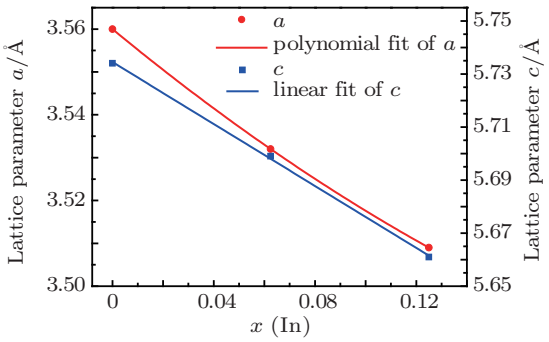


Fig. 3. (color online) Composition dependences of the calculated lattice constants a (a) and c (b) of $In_{1-x}Ga_xN$ alloy. The circles show the lattice parameter a of $In_{1-x}Ga_xN$ alloy. The diamonds show the lattice parameter c of $In_{1-x}Ga_xN$ alloy.

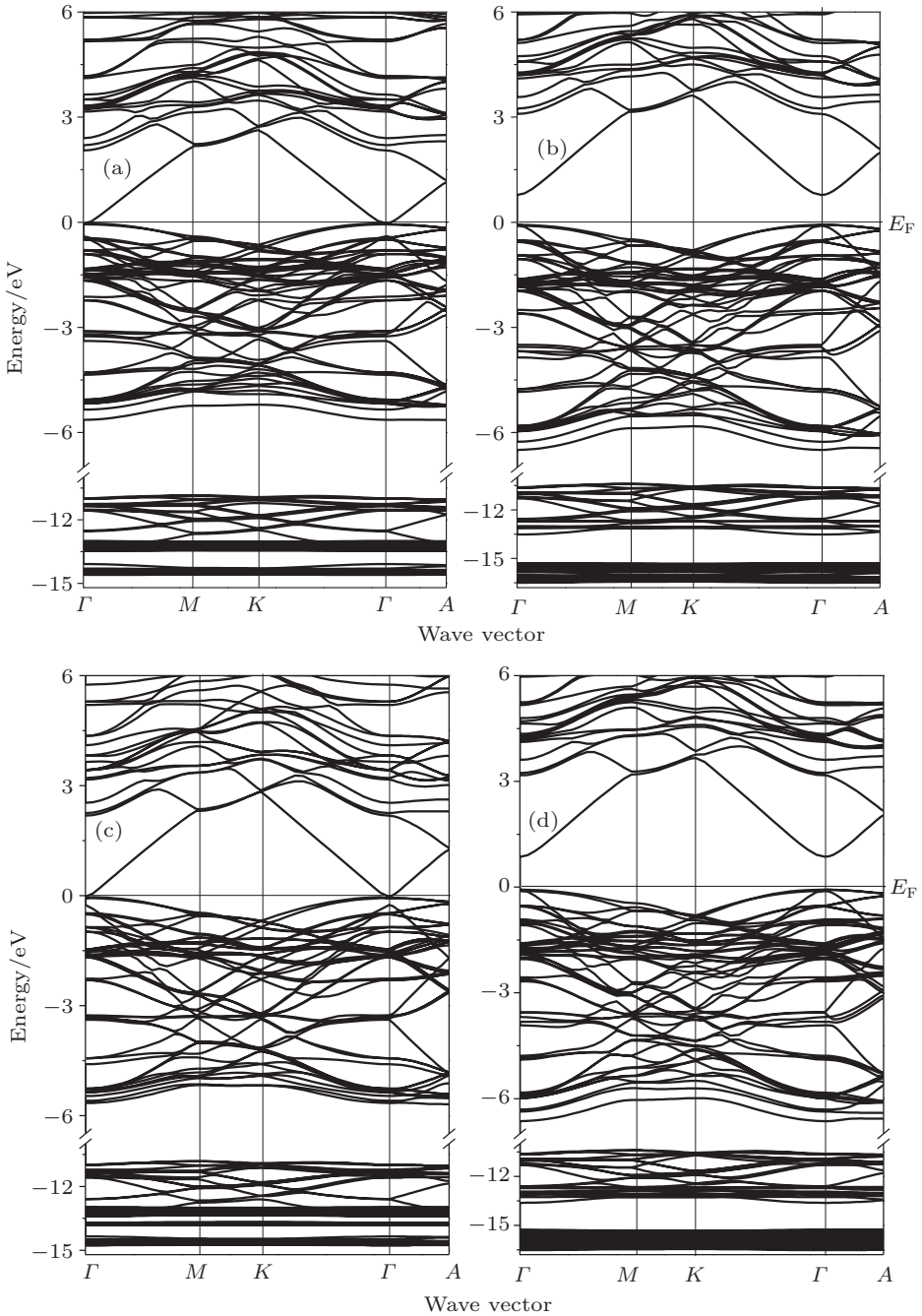


Fig. 4. Band structures of $In_{1-x}Ga_xN$ using GGA (a) and GGA + $U^{(d+p)}$ (b) for $x = 0.0625$, and band structures of $In_{1-x}Ga_xN$ using GGA (c) and GGA + $U^{(d+p)}$ (d) for $x = 0.125$.

Table 2. Comparison between the predicted values of band gap, the up-VB and low-VB with gallium concentration $x = 0$, 0.0625, 0.125 and experimental data.

	GGA			GGA + $U^{(d+p)}$			EXP.		
x	band gap/eV	up-VB/eV	low-VB/eV	band gap/eV	up-VB/eV	low-VB/eV	band gap/eV	up-VB/eV	low-VB/eV
0	0.0125	5.42	3.594	0.78	6.24	5.83	0.69	6.0	
0.0625	0.032	5.64	3.612	0.85	6.42	5.89	0.84[h]		
0.125	0.043	5.96	3.756	0.92	6.57	5.92	0.94[h]		

[h]Ref. [30].

3.3. Density of states and projected density of states of $In_{1-x}Ga_xN$

In order to further understand the phenomena in Subsection 3.2, the total densities of states (TDOSs) and the projected densities of states (PDOSs) are calculated for $In_{1-x}Ga_xN$ with x equal to 0, 0.0625, and 0.125, respectively, and shown in Figs. 5(a), 5(b), and 5(c), where all the tops of the valence bands are chosen as the Fermi energy level. The increases in the band-gap and valence-band width stem from the repulsion of p–d electrons,[31] and the detailed formulations are as follows:[31]

$$\varepsilon_{\rm pd}^{\rm ab} - \varepsilon_{\rm pd}^{b} = E = 2\left[\frac{\left(\varepsilon_{\rm p} - \varepsilon_{\rm d}\right)^2}{4} + V_{\rm pd}^2\right]^{1/2}, \tag{3}$$

$$Q_{\rm d} = 1 - \left[1 + \left(\frac{\Delta E_{\rm pd}}{V_{\rm pd}}\right)^2\right]^{-1}, \tag{4}$$

$$E = \left(\varepsilon_{\rm p} - \varepsilon_{\rm d}\right) + 2\Delta E_{\rm pd}, \tag{5}$$

$$\Delta E_{\rm pd} \sim \frac{V_{\rm pd}^2}{\varepsilon_{\rm p}^{a} - \varepsilon_{\rm d}^{c}}, \tag{6}$$

where E is a function of $[\Gamma_{15v}(\rm pd)$–$\Gamma_{15d}(\rm dp)]$; $\Delta E_{\rm pd}$ is the offset of p–d repulsion energy which is obtained by comparing the calculated total valence-band width when d states are included and the width obtained in the absence of d bands; $Q_{\rm d}$ is the fractional d charge in the anti-bonding $\Gamma_{15v(\rm pd)}$; $\Gamma_{15v} - \Gamma_{15d}$ is the valence band width. The valence band maximum (VBM) is influenced by $\Delta E_{\rm pd}$. $Q_{\rm d}$ and $\Gamma_{15v} - \Gamma_{15d}$ are determined by the electronegativity of p and d, the difference in p and d orbital of valence electron, and the radius of the valence electron. If $\Delta E_{\rm pd}$ is reduced, the p–d repulsion will be weakened and the anion-p electronic orbit shifts toward the lower energy states. The VBM of GaN has a smaller value than that of InN, so that the repulsion between Ga–3d and N–2p is weaker than the repulsion between In–4d and N–2p. Furthermore, the offset of InN/GaN is small and only has a value of 0.15 eV, which accords well with the experimental result.[32]

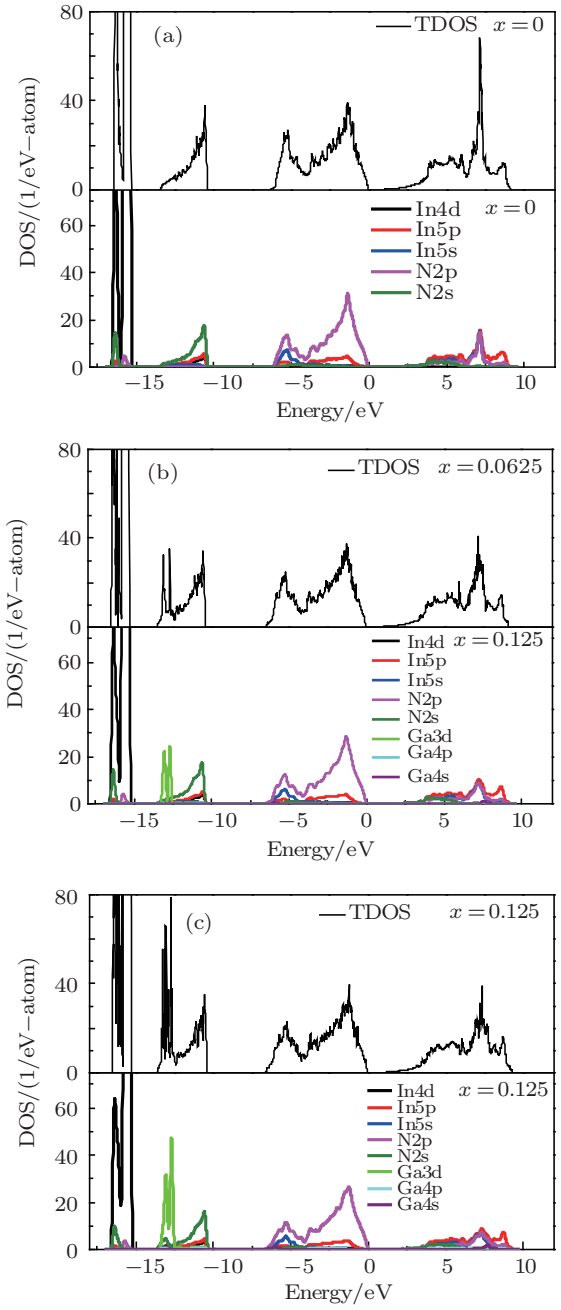


Fig. 5. (color online) Calculated TDOSs and PDOSs of $In_{1-x}Ga_xN$ for $x = 0$ (a), $x = 0.0625$ (b), and $x = 0.125$ (c).

Figure 6 shows the calculated PDOSs of the indium atom and gallium atom for the $In_{1-x}Ga_xN$ alloys with gallium concentrations of 0, 0.0625, and 0.125. It can be seen in Fig. 6 that the Ga–4p, In–5p, and Ga–4s, In–5s have the same main

peak positions for the same Ga concentration. The state density distributions from Ga–4p, In–5p, and Ga–4s, In–5s shift toward the conduction band in the high energy direction. It is shown that the strong hybridizations of the Ga–4p, In–5p, and Ga–4s, In–5s electrons are due to the similar forms of the PDOS distributions.

In summary, the increases in the band-gap and valence band width show that an anti-Stokes shift occurs with the band-gap variation due to the composition fluctuations.[33] It also reveals that the In-atoms and Ga-atoms are more electropositive, and strong ionization of the nitrogen atoms can be expected.[34]

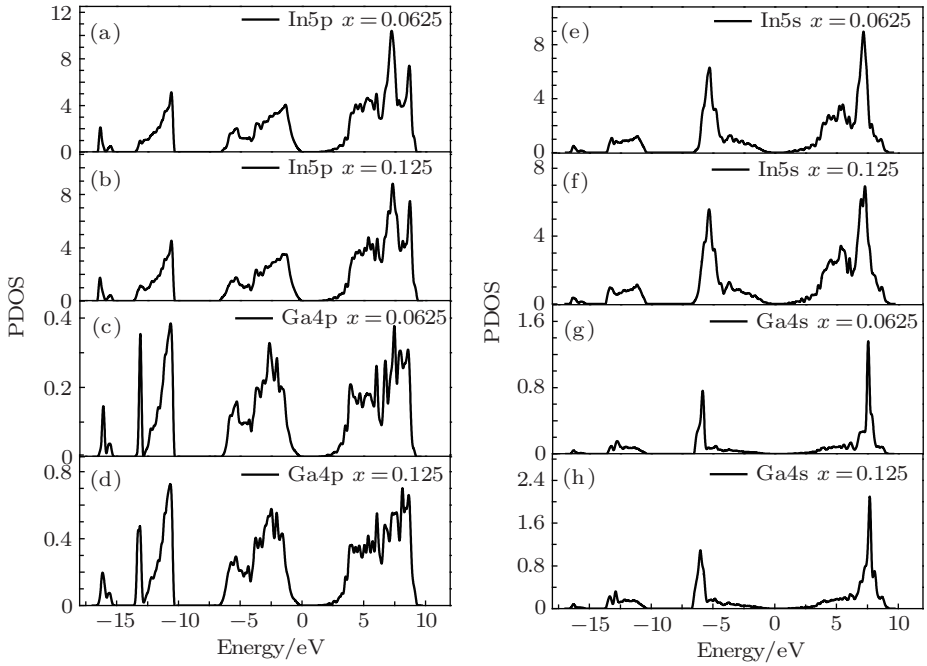


Fig. 6. Calculated PDOSs of In–5p and Ga–4p electronic states for $x = 0.0625$, $x = 0.125$ (panels (a)–(d)) respectively; PDOSs of In–5s and Ga–4s electronic states for $x = 0.0625$, $x = 0.125$ (panels (e)–(h)) respectively.

4. Conclusions

The electronic band structures DOSs, and PDOSs are studied of the wurtzite $In_{1-x}Ga_xN$ with $x = 0$, 0.0625, 0.125 by the GGA and GGA + $U^{(d+p)}$ in the density function theory which includes In–4d and Ga–3d electronic states. Our results are compared with GGA and experimental data. The results are surprisingly fine. The GGA + $U^{(d+p)}$ of predictions about the band gap and the valence-band width remarkably fit well with the experimental results for the wurtzite $In_{1-x}Ga_xN$. The band-gap and valence band width of $In_{1-x}Ga_xN$ increase with Ga concentration increasing. It is confirmed that the increases of the band gap and the valence-band width stem from the repulsion of p–d electrons and strong hybridizations of the Ga–4s, In–5s, and Ga–4p, In–5p electrons. Furthermore, the compressive strain in the crystal can cause the band-gap and valence band width to increase with gallium content x increasing.

References

[1] Liu C, Ren Z W, Chen X, Zhao B J, Wang X F, Yin Y A and Li S T 2013 *Chin. Phys. B* **22** 058502

[2] Aschenbrenner T, Dartsch H, C. Kruse, Anastasescu M, Stoica M, Gartner M, Pretorius A, Rosenauer A, Wanger T and Hommel D 2010 *J. Appl. Phys.* **108** 063533

[3] Zhang K, Cao M Y, Chen Y H, Yang L Y, Wang C, Ma X H and Hao Y 2013 *Chin. Phys. B* **22** 057304

[4] Shan W, Walukiewicz W, Haller E E, Little B D, Song J J, McCluskey M D, Johnson N M, Feng Z C, Schurman M and Stall R A 1998 *J. Appl. Phys.* **84** 4452

[5] Sanford N A, Munkholm A, Krames M R, Shapiro A, Levin I, Davydov A V, Sayan S, Wielunski L S and Madey T E 2005 *Phys. Stat. Sol. (c)* **7** 2783

[6] Yildiz A, Oŭtuŕk M K, Bosi M, Oŭçelik S and Kasap M 2009 *Chin. Phys. B* **18** 4007

[7] Zhang X Y, Chen Z W, Qi Y P, Feng Y, Zhao L, Qi L, Ma M Z, Liu R P and Wang W K 2007 *Chin. Phys. Lett.* **24** 1032

[8] Furthmüller J, Hahn P H, Fuchs F and Bechstedt F 2005 *Phys. Rev. B* **72** 205106

[9] Maurya T K, Kumar S and Auluck S 2010 *Opt. Commun.* **283** 4655

[10] Cococcioni M and de Gironcoli S 2005 *Phys. Rev. B* **71** 035105

[11] Vladimir I A, Jan Z and Ole K A 1991 *Phys. Rev. B* **44** 943

[12] Terentjevs A, Catellani A, Prendergast D and Cicero G 2010 *Phys. Rev. B* **82** 165307

[13] Perdew J P, Burke K and Ernzerhof M 1996 *Phys. Rev. Lett.* **77** 3865

[14] Giannozzi P, Baroni S, Bonini N, Calandra M, Car R, Cavazzoni C, Ceresoli D, Chiarotti G L, Cococcioni M, Dabo I, Corso A D, de Gironcoli S, Fabris S, Fratesi G, Gebauer R, Gerstmann U, Gougoussis C, Kokalj A, Lazzeri M, Martin-Samos L, Marzari N, Mauri F, Mazzarello R, Paolini S, Pasquarello A, Paulatto L, Sbraccia C, Scandolo S, Sclauzero G, Seitsonen A P, Smogunov A, Umari P and Wentzcovitch R M 2009 *J. Phys.: Condens. Matter* **21** 395502

[15] Butcher K S A and Tansley T L 2005 *Superlattice and Microstructures* **38** 1
[16] Methfessel M and Paxton A T 1989 *Phys. Rev. B* **40** 3616
[17] Kokalj A 2003 *Comput. Mater. Sci.* **28** 155
[18] Janotii A, Segev D and Van de Walle C G 2006 *Phys. Rev. B* **74** 045202
[19] Korotin M, Fujiwara T and Anisimov V 2000 *Phys. Rev. B* **62** 5696
[20] King P D C, Veal T D, McConvile C F, Fuchs F, Furthmüller J, Bechstedt F, Schörmann J, As D J, Lischka K, Lu H and Schaff W J 2008 *Phys. Rev. B* **77** 115213
[21] Furthmüller J, Hahn P H, Fuchs F and Bechstedt F 2005 *Phys. Rev. B* **72** 205106
[22] Christensen N E and Gorczyca I 1994 *Phys. Rev. B* **50** 4397
[23] Zhang S, Shi J J, Zhu S G, Wang F, Yang M and Bao Z Q 2010 *Phys. Lett. A* **374** 4767
[24] Stampfl C and Van de Walle C G 1999 *Phys. Rev. B* **59** 5521
[25] Yeo Y C, Chong T C and Li M F 1997 *J. Appl. Phys.* **83** 1429
[26] Liou B T, Lin C Y, Yen S H and Kuo Y K 2005 *Opt. Commun.* **249** 217
[27] Gavrilenko V I and Wu R Q 2000 *Phys. Rev. B* **61** 2632
[28] Wu J, Walukiewicz W, Shan W, Yu K M and Ager J W 2003 *J. Appl. Phys.* **94** 4457
[29] Piper L F, Veal T D, Jefferson P H and McConville C F 2005 *Phys. Rev. B* **72** 245319
[30] Wu J, Walukiewicz W, Yu K M, Ager J W and Haller E E 2002 *Appl. Phys. Lett.* **80** 4741
[31] Wei S H and Zunger A 1988 *Phys. Rev. B* **37** 8958
[32] Wei S H and Zunger A 1998 *Appl. Phys. Lett.* **72** 2011
[33] Ferhat M, Furthmüller J and Bechstedt F 2002 *Appl. Phys. Lett.* **80** 1394
[34] Tit N 2010 *J. Alloys Compd.* **503** 529